

Copyright notice:

Copyright 2013 Society of Photo-Optical Instrumentation Engineers. One print or electronic copy may be made for personal use only. Systematic reproduction and distribution, duplication of any material in this paper for a fee or for commercial purposes, or modification of the content of the paper are prohibited.

Citation:

Matthew C. George ; Bin Wang ; Romyana Petrova ; Hua Li, Jonathan Bergquist, " Nanowire grid polarizers for mid- and long-wavelength infrared applications", Proc. SPIE 8704, Infrared Technology and Applications XXXIX, Bjørn F. Andresen; Gabor F. Fulop; Charles M. Hanson; Paul R. Norton, Vol. 8704, 87042E, (2013).

DOI abstract link:

<http://dx.doi.org/10.1117/12.2016221>

Nanowire grid polarizers for mid- and long-wavelength infrared applications

Matthew C. George*, Bin Wang, Rumyana Petrova, Hua Li, Jonathon Bergquist
Moxtek Inc., 452 W 1260 N, Orem, UT, USA;

ABSTRACT

High contrast wire grid polarizers on silicon suitable for mid-wavelength infrared (MWIR) and long-wavelength infrared (LWIR) applications have been developed using wafer-scale aluminum nanowire patterning capabilities. The 144 nm pitch MWIR polarizer typically transmits better than 95% of the passing polarization state from 3.5-5.5 microns while maintaining a contrast ratio of better than 37dB. Between 7 and 15 microns, the broadband LWIR polarizer typically transmits between 55 and 90% of the passing state and has a contrast ratio better than 40 dB. A narrowband 10.6 micron polarizer shows about 85% transmission in the passing state and a contrast ratio of 45 dB. Transmission and reflection measurements were made using various FTIR spectrometers and compared to RCWA modeling of the wire grid polarizer (WGP) performance on antireflection-coated wafers. Laser Damage Threshold (LDT) testing was performed using a continuous wave CO₂ laser for the broadband LWIR product and showed a damage threshold of 110 kW/cm² in the blocking state and 10 kW/cm² in the passing state. The MWIR LDT testing used an OPO operating at 4 microns with 7 ns pulses and showed LDT of 650 W/cm² in the blocking state and better than 14 kW/cm² in the passing state.

Keywords: wire grid polarizer, nanofabrication, sub-wavelength optics, form birefringence, laser damage threshold, MWIR, LWIR, thermal IR

1. INTRODUCTION

The wire grid polarizer (WGP) remains one of the most useful optical components in the field and is prevalent in applications ranging from imaging and displays to communications and scientific instrumentation. The WGP typically consists of an array of metallic lines with sub-wavelength pitch supported by a transparent substrate. Wire grid structures are known to be effective as infrared polarizers with short optical path and large acceptance angles.¹⁻² Existing WGP products designed for mid-wavelength IR and long-wavelength thermal IR applications typically suffer from low contrast between transmission of linearly polarized light in the passing and blocking configurations, which is due to their relatively large wire grid pitch (typically ≥ 370 nm). Moxtek and others have previously demonstrated a large increase in aluminum WGP performance at visible and ultraviolet wavelengths by reducing the pitch.³⁻⁴ It follows that a dramatic reduction in pitch from that found in typical IR WGP products should greatly improve mid- and long-wavelength IR contrast. Moxtek has therefore developed several high contrast IR polarizers on anti-reflection (AR) coated silicon suitable for mid-wavelength IR (MWIR) and long-wavelength IR (LWIR) applications using wafer-scale aluminum nanowire patterning capabilities. The MWIR polarizer transmits better than 95% of the passing state between 3.5 and 5.5 microns while maintaining a contrast ratio of better than 37dB from 3-7 microns, while the broadband LWIR polarizer transmits between 55% and 90% of the passing polarization state between 7 and 15 microns and has a contrast ratio exceeding 40 dB. A narrowband polarizer for 10.6 microns is also being developed and shows 85% transmission in the passing state and a contrast ratio of about 45 dB.

Figure 1 depicts Moxtek aluminum WGP products on silicon and glass substrates and demonstrates wafer-scale processing capability. The infrared AR coatings for silicon can be custom designed to provide enhanced transmission for narrowband or broadband applications. The fine pitch (144 nm) and large rib aspect ratio ($> 3:1$) provide for improved transmission and dramatically higher contrast than competing WGP products. Potential applications for the MWIR and LWIR polarizers include spectroscopic measurement systems, optical isolators for industrial lasers, and polarization sensitive imaging systems for hyperspectral imaging, guided missile technology, and forward-looking infrared thermal imaging. With the increasing use of lasers in polarization-sensitive industrial and scientific applications, laser damage threshold (LDT) testing has also been pursued for these WGP products.

*mgeorge@moxtek.com;

phone

1

801

225-0930;

www.moxtek.com

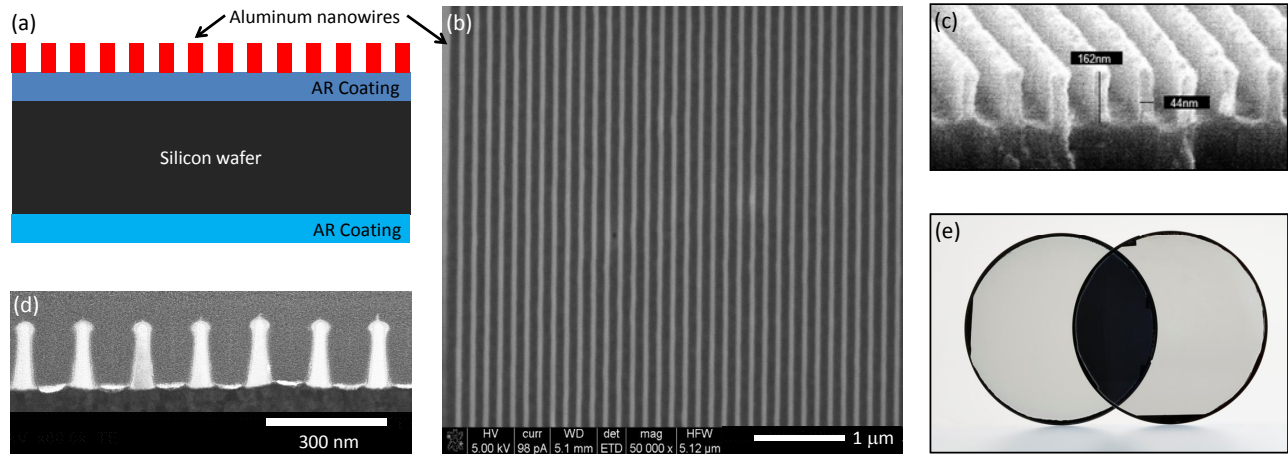


Figure 1. Moxtek Wire Grid Polarizers. (a) Schematic of wafer cross section (not to scale). (b)-(c) SEM images of aluminum nanowires on MWIR AR-coated silicon in (b) Plan view and (c) cross-section. (d) STEM image of rib cross-section for LWIR product after embedding in Platinum and focused ion beam milling to remove a thin section for imaging. (e) Photograph of crossed 144 nm pitch aluminum nanowire grid polarizers on 200 mm diameter glass wafers, depicting Moxtek wafer scale processing capabilities.

2. METHODOLOGY

2.1 Overview

Fourier Transform Infrared (FTIR) spectroscopic analysis of part performance in transmission was completed at Moxtek and verified at an outside reference lab. Open and blocked beam configurations and a silicon reference standard were used to validate instrument accuracy for transmission measurements. Results were validated at a third lab by fixed wavelength transmission measurements using a CO₂ laser centered at 10.6 μm and an OPO operating at 4 μm. Laser Damage Threshold measurements were also completed in the passing and blocking polarizer orientations. FTIR analysis of part performance in reflectance was completed internally and at an outside reference lab using an absolute specular reflectance accessory, but maintaining polarization purity was a challenge. Optical modeling of part performance was undertaken using the rigorous coupled wave analysis (RCWA). Sample analysis was performed using scanning electron microscopy (SEM), focused ion beam (FIB) milling, and scanning transmission electron microscopy (STEM).

2.2 FTIR transmission experiments

Figure 2a depicts the experimental setup for normal incidence transmission measurements. A Cary 670 FTIR spectrometer was used with a fixed pre-analyzer consisting of two Moxtek polarizers on silicon spaced by several millimeters, and containing the same double-sided AR coatings as the product being measured. After nitrogen purging for 5-10 minutes, a background scan was taken without a sample in the compartment to establish the 100% transmittance baseline. The sample was then placed on a rotary stage and the broadband FTIR interferogram signal minimized to establish the blocking state polarizer orientation. After purging and measurement of the blocking state transmittance, the sample was rotated 90° and re-purged before recording the passing state transmittance. The sample was then removed and the purged background re-measured to ensure minimal baseline drift in the single beam FTIR instrument. Blocking the beam with a metal plate established the noise floor. To ensure ordinate accuracy in the intermediate transmission ranges, a bare (uncoated) silicon reference sample was also scanned and compared to transmittance models generated from IR variable angle spectroscopic ellipsometry (IR-VASE) analysis performed by the J.A. Woollam Company. The transmission experiments were also repeated at Ball Aerospace's Optical Testing Facility using a Nexus 870 FT-IR ESP spectrometer from Thermo Nicolet and showed the same nominal behavior in the passing state and blocking states. 256 scans were averaged per spectra in the blocking polarizer configuration to achieve sufficient dynamic range to measure a contrast ratio of 10,000 with a signal to noise ratio of 5:1.

2.3 FTIR reflection experiments

Reflectance measurements were initially performed at Ball Aerospace's Optical Testing Facility using the Thermo Nicolet FTIR spectrometer described previously as well as a Harrick specular reflectance accessory with 12° and 45° absolute reflectance stages and a broadband WGP on KRS-5 substrate as the pre-analyzer. The specular reflectance accessory imparts a small rotation on the incoming polarization state, but for the 12° absolute reflectance stage, this polarization state is maintained between the first and second sample reflections if the sample is isotropic. For a non-isotropic medium like a WGP, the input polarization state must be rotated using a pre-analyzer to give pure *p*- or *s*-type reflections from the sample or else there will be a more complicated convolution of *p*-type, *s*-type, passing-state, and blocking-state reflectance. The 45° reflectance stage does not maintain the same polarization state between the two bounces off the sample in the "W" configuration, thus a more complicated weighting of modeling results would be necessary to make quantitative comparisons between measurements and theoretical modeling.

The rotation of the input polarization state was not properly compensated for in the earlier measurements, thus the 12° angle of incidence (AOI) reflectance measurements were repeated at Moxtek using a Cary 670 FTIR spectrometer and the same Harrick reflectance accessory and stage. The same pre-analyzer described in the transmission measurements was used on a rotation mount to tune the input polarization state, which should allow for absolute measurements of R_p^2 and R_s^2 . The WGP sample was placed with the part edge against the bottom reference edge of the reflectance stage such that the wires were oriented up-and-down in the laboratory reference frame. This wire orientation is orthogonal to the plane of incidence, giving *s*- and *p*-reflections for the blocked and passing polarization states respectively. The stage was placed in the "V" configuration so that beam was *transmitted* through the sample twice, then the input polarization was tuned to the blocking state by rotating the pre-analyzer to minimize the FTIR detector signal. After removing the sample, a N₂-purged baseline was taken in the "V" beam path configuration. The sample was then placed back on the reflectance stage and the kinematic mount flipped to generate the "W" beam path configuration (figure 2b) for measurement of the reflectance-squared in the blocking state (R_s^2). The pre-analyzer was rotated 90° for passing state reflectance measurements (R_p^2) and the sample removed for a final corrective baseline in the "V" configuration. The reflectance of an uncoated piece of double-side-polished silicon was also measured to verify instrument accuracy.

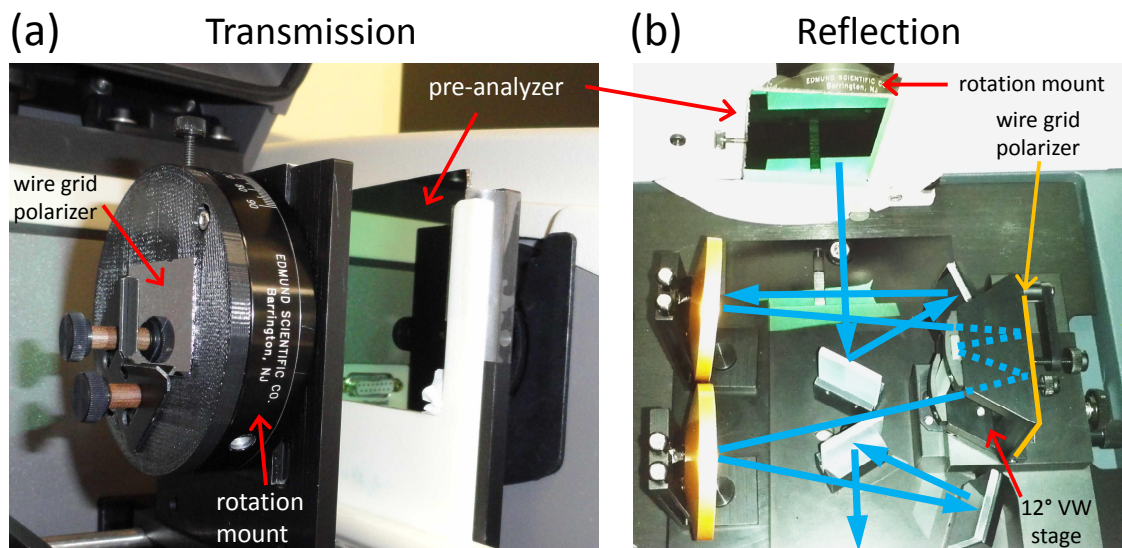


Figure 2. Measurement setups for FTIR spectroscopy in (a) transmission and (b) 12° reflection. The pre-analyzer, a doubled Moxtek AR-coated product, gives broadband linearly polarized light of high purity. The rotation mount allows for fine-scale alignment of the relative orientation of the WGP and pre-analyzer. In transmission (a), a reference scan is recorded, and then the sample is added and aligned by nulling the FTIR interferogram for a blocking state transmittance measurement. The part is then rotated 90° to measure the passing-state transmittance. In reflection (b) the pre-analyzer is first rotated to minimize the interferogram with the 12° VW stage in the V-configuration (two passes through sample) and then a reference scan is taken after then removing the sample. The blocking state R_s^2 measurement is taken after adding the sample and rotating the reflectance stage to the W-configuration. Then the pre-analyzer is rotated approximately 90° to measure R_p^2 and the sample removed for a final corrective baseline in the V-position. The sample chamber is purged with N₂ for all measurements.

2.4 Laser damage threshold testing

For the broadband LWIR product, laser damage threshold testing was performed at a wavelength of 10.6 μm using a continuous wave Synrad Firestar CO₂ laser at Spica Technologies, Inc. The beam was focused using a convex ZnSe lens (1 meter focal length) to a 360 μm $1/e^2$ spot size with a Rayleigh length of approximately 2 mm. The beam profile was measured using a calibrated aperture approach. The polarization purity of the laser beam was improved using a thin film plate polarizer designed for 10.6 μm wavelength. The beam was steered using zero-phase reflector mirrors and the laser power was attenuated using the reflective thin film plate polarizer and a partial reflector. Fine-tuning of laser output power was achieved using RF carrier wave modulation. Operating the laser at low powers led to increased carrier wave modulation of the instantaneous laser power and LDT behavior approaching that of a pulsed laser experiment. The CO₂ laser was thus operated at high power to reduce the spikes in the beam fluence and more faithfully characterize the continuous wave LDT of the product. The samples were tested with the aluminum ribs facing the incoming laser beam. Images of the sample surface were recorded before and after laser exposure using a 100x reflective microscope with Nomarski objective and examined for signs of laser damage. Damage was also identified by monitoring the power passing through the LWIR polarizer using a Laser Precision Meter Rk-5720 power ratiometer with Laser Probe Rk-570 pyroelectric power head and integrated chopper. An Ophir 150C-sh thermopile detector head with SH-USBI interface was used to measure incident laser power and passing-state transmittance. High LWIR polarizer contrast was verified using the same laser source and detectors. For the MWIR product, a Spectra Physics 1064nm HIPPO laser operating at 25 kHz was used to pump a PPLN OPO for 7 ns pulses at a wavelength of 4 μm . The $1/e^2$ beam diameter was varied from 370 μm for the blocking state LDT measurement and reduced to 95 μm for the passing state measurement.

2.5 Sample analysis

Samples were characterized in plan-view and cross-section by SEM. It was found that a further investigation of the cross-sections by STEM was needed for improved resolution of the finer-scale sample features. Cross sectional STEM lamellae were prepared by a focused ion beam (FIB) in-situ lift-out technique using an FEI Nova 200 Dual Beam instrument. Samples were then observed in bright and dark field using a Hitachi HD-2000 STEM instrument operating at 200 kV. Platinum infiltration was performed before the FIB milling to protect the delicate wire grid structure from beam damage.

2.6 Optical modeling

Rigorous Coupled Wave Analysis (GSolver[®] version 4.20b) was utilized in optical modeling of the silicon IR products. The model incorporated silicon IR optical constants generated by J.A. Woollam from IR-VASE and transmittance analysis of a series of uncoated silicon parts. The model also utilized aluminum optical constants derived from an earlier J.A. Woollam IR analysis based on a generic oscillator model. AR coating data provided by Universal Thin Film Lab Corp. was also input into the optical model to account for the reduced silicon reflectivity. For modeling purposes a simple rectangular wire cross section was assumed, with the metal duty cycle fixed at 27.8% (40 nm) of the wire grid pitch (144 nm). The wire height was set to 165 nm, giving an aspect ratio of about 4.1 to 1. In addition to the real zero order propagating modes, convergence of the RCWA solutions was observed with inclusion of only +/- 12 reflected and +/-12 transmitted evanescent diffracted orders. Transmission simulations were performed by multiplying the zero order transmittance of two different models. The first utilized a semi-infinite air superstrate followed by the WGP layer, ARC layers, 0.62 mm thick silicon layer, and a semi-infinite silicon substrate. These transmittance results include all front-side wafer surface reflections as well as absorption from the WGP, top ARC layers, and the Silicon substrate. The second model utilized the same semi-infinite superstrate and semi-infinite substrate with ARC layers in-between and accounts for the reflective losses from the backside of the wafer. Coherent effects between front and backside wafer reflections are ignored. For reflectance modeling, the backside wafer reflectance was ignored as it is small within the ARC design region. For the modeling at varying AOI, the s-type reflection was chosen such that the polarization direction is aligned with the wires while the p-type reflection is orthogonal to the wires, hence R_s is the blocking state reflectance while R_p is the passing state reflectance. This nomenclature not only provides a distinction for the normal incidence reflections, but the configuration gives improved performance in polarizing beam-splitter applications.

3. MEASUREMENT RESULTS AND DISCUSSION

3.1 Overview

FTIR transmission analysis of Moxtek IR polarizers showed excellent contrast results between blocking and passing states (>37 dB over the design wavelengths). For the MWIR product, passing state transmission was typically very high (>95%) over the AR-coating design region. AR-coating defects and silicon IR absorption limited the passing state transmission for the broadband LWIR product to a range of 55-90% for the 7-15 μm design region. A narrowband polarizer for 10.6 μm showed 85% transmission in the passing state and a contrast ratio of about 45 dB. RCWA modeling results for normal incidence transmission and 12° angle of incidence reflectance of the broadband MWIR and LWIR polarizers matched the general trends observed in the corresponding FTIR experiments. For the broadband LWIR product, preliminary LDT testing indicates that damage is being initiated at defects introduced during silicon AR coating. In the blocking state, the LWIR product can withstand 110 kW/cm^2 of continuous wave CO_2 laser radiation at 10.6 μm wavelength, while the parts show an order of magnitude lower laser damage threshold in the passing polarization state. The Moxtek MWIR polarizer has an improved AR coating and does not show the same damage initiation mechanism. The MWIR product showed a LDT of 650 W/cm^2 in the blocking state and better than 14 kW/cm^2 in the passing state at a wavelength of 4 μm .

3.2 FTIR transmission experiments

Figure 3 depicts FTIR normal incidence passing-state transmission measurement results for LWIR and MWIR products as well and the calculated contrast ratios between passing and blocking states. The corresponding optical modeling results described in section 3.6 are also plotted for comparison. Transmission of the passing polarization state for the MWIR product is better than 95% between 3.5 and 5.5 μm . The best performing LWIR sample (labeled experimental T_p) transmits between 73 and 92% in the AR coating design region, although more typical performance spans the 57-75% range, depending on wavelength. A narrowband polarizer designed for 10.6 μm wavelength CO_2 laser applications gave over 85% transmittance in the passing state. The Moxtek LWIR polarizer performance in the passing state is currently limited by the silicon substrate thickness (due to IR absorption features) and the AR coating performance. The FTIR instrument noise floor limited transmission measurement in the blocking state, but the maximum measurable contrast ratio (5:1 signal to noise) was still better than 40 dB between 3 and 15 microns for the Nexus 870 using 256 scan averaging and slightly better for the CARY 670. The MWIR product maintained a contrast ratio of better than 37dB from 3-7 μm , while the best LWIR samples had an average contrast ratio of about 43.5 dB from 7-15 μm . High contrast for the broadband LWIR product was verified at Spica Technologies using laser sources and showed contrast ratios ranging from 40.5 to 48.1 dB at 10.6 μm wavelength with a typical contrast of about 45 dB. The narrowband 10.6 μm polarizer was analyzed with the CARY 670 FTIR and also showed a contrast ratio of about 45 dB.

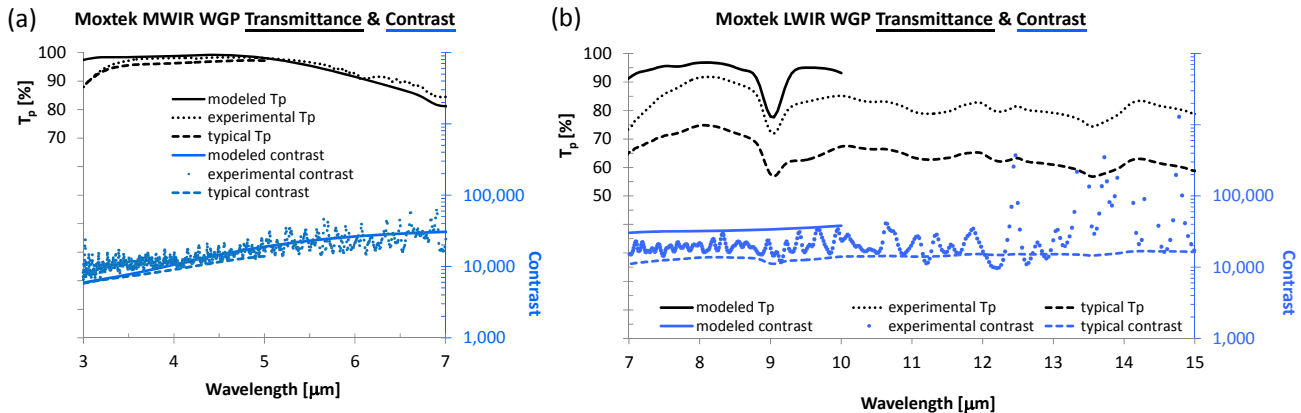


Figure 3. Normal incidence transmittance and contrast ratio for (a) MWIR and (b) LWIR broadband polarizers. The dotted and dashed lines and data points are based on FTIR measurements while the solid lines represent optical modeling results. The **black** data represents the **transmittance** of light polarized orthogonal to the wire grid direction (passing state) and uses the transmittance scale on the left, while the **blue** data corresponds to the **contrast ratio** between passing/blocking polarizer states and uses the log scale ordinate on the right. The *typical* curves are based on the best fit to passing and blocking state transmittance measurements from many samples while the *experimental* data points are for the best performing samples.

3.3 FTIR reflection experiments

Figure 4 presents polarizer reflectance measurements at 12° angle of incidence (AOI) using the CARY 670 FTIR and Harrick absolute specular reflectance accessory, as well as modeling results discussed in section 3.6. Proper tuning of the input polarization state allows for R_p^2 and R_s^2 to be directly measured at 12° AOI, as described in section 2.3. Much of the slight disagreement between modeling and theory is likely a result of improper pre-analyzer alignment. According to Harrick Scientific,⁵ vertically polarized light is rotated differently than horizontally polarized light through their specular reflectance accessory. Since fine alignment of the pre-analyzer orientation was only performed for the R_s^2 measurement, the R_p^2 measurements evidently had a beam polarization that was rotated slightly (~10°) from the optimal orientation. The “VW” method for R^2 measurements also assumes that there is no depolarization of the beam by the sample in reflectance, which is only true if the pre-analyzer is properly aligned and the beam is of high purity. Although the aluminum beam steering mirrors of the Harrick accessory have only a weak dependence on polarization orientation, this depolarization effect will also bias the second sample reflection further towards the s-polarization state. These factors help explain why the R_p measurements are slightly larger than the modeling results. The reduced R_s in figure 4b of the Moxtek LWIR polarizer compared to modeling could be due to scattering from defects in the AR coating or from improper sample mounting. Reflectance measurements at 45° AOI were also taken for MWIR and LWIR products, but due to the sample and alignment dependent mix of *s*- and *p*-type and blocking- and passing-state reflections, quantitative comparison between modeling and experiment was not undertaken.

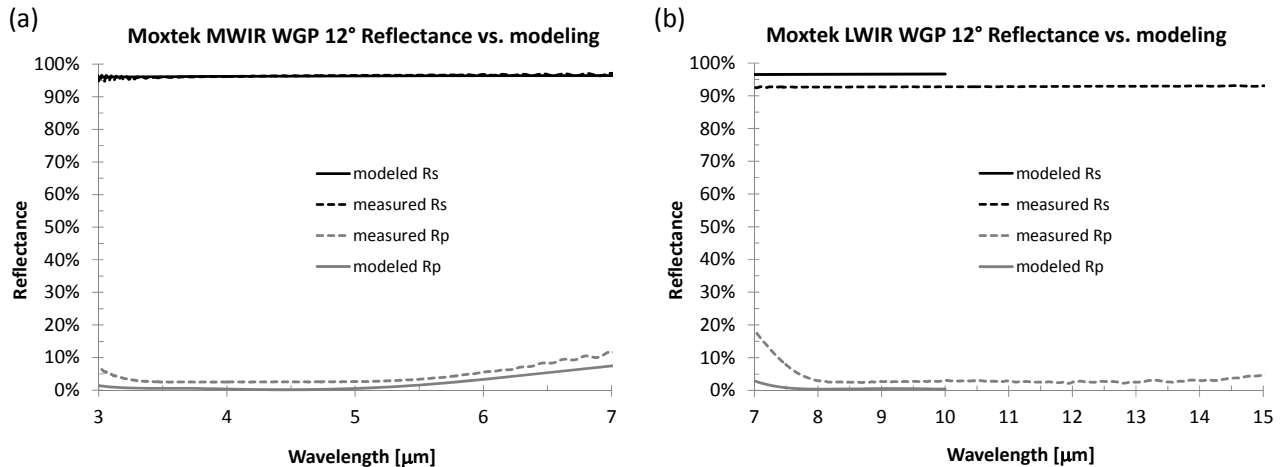


Figure 4. FTIR 12° angle of incidence reflectance measurement results for (a) MWIR and (b) LWIR products. Solid and dashed lines denote reflectance modeling and experimental measurements respectively. **Black** lines indicate *s*-type reflections in the blocking polarizer state and **grey** lines indicate *p*-type reflections in the passing polarizer state (with slight misalignment in the *p*-type measurement case).

3.4 Laser damage threshold testing

For the MWIR product, preliminary pulsed laser damage threshold testing at 4 μm wavelength indicated the wires can withstand 650 W/cm² in the blocking state and better than 14 kW/cm² in the passing state. For the broadband LWIR product, preliminary continuous wave laser damage threshold testing at 10.6 μm indicates that defects introduced during silicon AR coating are limiting performance. In the blocking state the wires can withstand 110 kW/cm² of continuous wave CO₂ laser radiation, while the parts show an order of magnitude lower laser damage threshold for the passing polarization state (10 kW/cm²). The damage appears to initiate and spread from defects in the AR coating. These samples were tested with the aluminum wires facing the incoming laser beam, and hence in the blocking configuration the wire grid should help protect the AR coating defects from laser damage as they reflect over 95% of the incident radiation. The MWIR polarizer had a defect-free AR coating and did not show the same damage initiation mechanism.

3.5 Sample analysis

From SEM and STEM images (figures 1c and 1d), it is evident that the etched aluminum wires do not have the rectangular cross section assumed in the optical modeling. From STEM analysis of the broadband LWIR product, the

wire width varied from about 30-60 nm over the cross section and the wire height was about 190 nm. STEM analysis of the MWIR product revealed a wire width varying from 25-55 nm over the cross section and a wire height of 160-165 nm. For simplicity all modeling assumed 40 nm wire width and 165 nm tall wires. A thin native aluminum oxide is also evident on the outside of the wires for both products, but was not modeled.

3.6 Optical modeling

To verify the accuracy of the optical modeling, the passing state transmittance and calculated contrast ratio between the passing and blocking polarizer orientations were plotted against the corresponding experimental data in figure 3a - 3b for the broadband MWIR and LWIR products respectively. The MWIR product shows good agreement between transmission modeling and measurements except at the shorter wavelengths. Interference fringes (not evident within the displayed range) appear at slightly shorter wavelengths in the broadband LWIR product modeling. LWIR modeling also shows larger average transmittance in the passing state when compared to the best experimental case. Errors in the fit could be due to the use of improper optical constant data in the infrared, the omission of native oxides from the modeling,² or the use of improper thickness for one or more simulation layer. Geometrical parameters such as metal wire width and shape are also approximated in the model by a rectangular cross section, which disagrees with the SEM and STEM analysis results. The silicon optical constants used in the modeling were based on an analysis of double-side polished silicon performed by J.A. Woollam using coupled IR-VASE and transmission measurements, and had a slightly lower value of IR index of refraction than the value extrapolated from the well-cited analysis of Herzinger et.al.⁶ For comparison, 12° AOI reflectance modeling results for broadband MWIR and LWIR products were plotted alongside the experimental measurements in figures 4a - 4b. As discussed in section 3.3, much of the slight disagreement between modeling and theory is likely a result of improper pre-analyzer alignment, but the modeling also neglects the backside reflection, which explains why the disagreement appears more pronounced at the extremes of the AR coating pass band.

Figures 5 presents the transmittance (5a) and contrast (5b) modeling results for both MWIR and LWIR broadband products at various AOI, with the data range currently limited at the longer wavelengths to 10 μm. The results show little difference in performance when moving away from normal incidence, although the pass band for the AR coating shifts to shorter wavelengths at larger AOI. Transmittance remains high for the passing state polarization, which should maintain system efficiency even when projecting or imaging IR sources through the polarizer at large angles. In imaging applications, a converging or diverging beam can be passed through these wire grid polarizers with only a slight decrease in intensity towards the edges of the beam at longer wavelengths for the MWIR product.

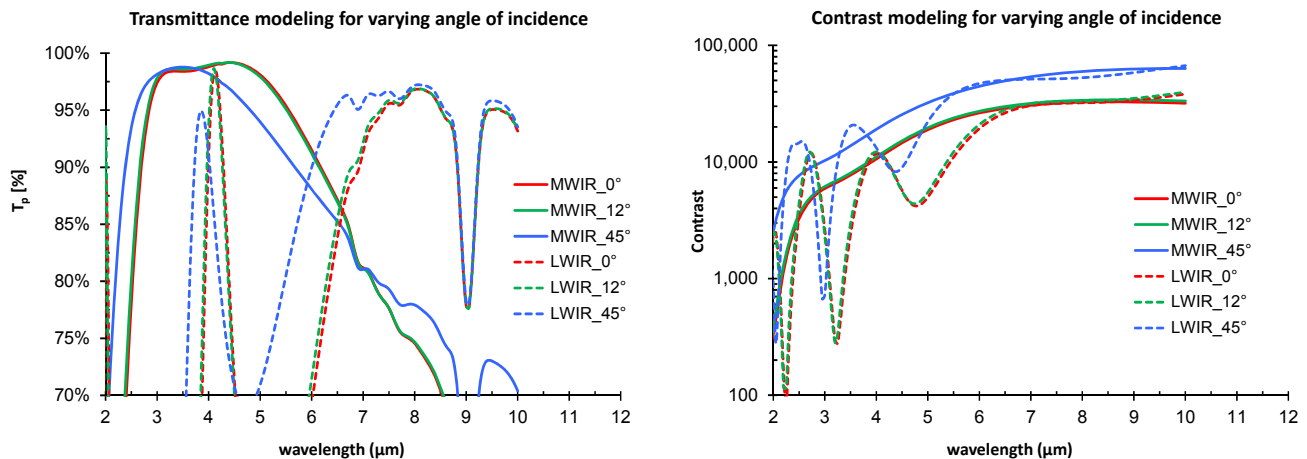


Figure 5. Optical modeling of (a) transmittance and (b) contrast ratio for MWIR (solid lines) and LWIR (dashed lines) broadband WGP products at varying angle of incidence (red – 0°, green – 12°, blue – 45°).

4. CONCLUSIONS

Moxtek has developed several high contrast IR polarizers on silicon suitable for mid-wavelength and long-wavelength thermal IR applications using wafer-scale aluminum nanowire patterning capabilities. Between 7 and 15 μm the broadband LWIR polarizer typically has between 55 and 90% passing state transmittance and maintains a contrast ratio of better than 40 dB. A narrowband product designed for the 10.6 μm CO₂ laser wavelength has better than 85% passing state transmittance and a contrast ratio of about 45dB. Moxtek has also developed a broadband MWIR polarizer that shows high contrast (>37 dB) between blocking and passing states and an exceptionally high passing state transmission (>95% between 3.5 and 5.5 μm). Transmission and reflectance measurements from a Fourier Transform Infrared spectrometer showed good qualitative agreement with optical modeling results from a rigorous coupled wave analysis package. Preliminary LDT testing and sample analysis indicated that laser damage was initiated at defects in the silicon AR coating for the LWIR product. The wires of the broadband LWIR product can withstand 110 kW/cm² of continuous wave CO₂ laser radiation at 10.6 μm wavelength in the blocking state, while the product shows an order of magnitude lower laser damage threshold for the passing polarization state. Removing the AR coating defects should improve LDT performance in the thermal IR and may also result in an increased transmittance in the passing configuration. The Moxtek MWIR polarizer has an improved AR coating and does not show the same LDT damage initiation mechanism. Pulsed laser damage threshold testing at a wavelength of 4 μm indicated the wires can withstand 650 W/cm² in the blocking state and better than 14 kW/cm² in the passing state.

REFERENCES

- [1] Goldstein, D.H., Erbach, P., "Evaluation of infrared (3-12 μm) wire grid polarizers", Proc. of SPIE 7672, 76720E (2010).
- [2] Hu, C. and Liu, D., "A high-performance Aluminum wire-grid polarizer for the optical telecommunication applications", Proc. of SPIE 7134, 71344J-6 (2008).
- [3] Wang, J.J., Walters, F., Liu, X., Sciortino, P. and Deng, X., "High-performance, large area, deep ultraviolet to infrared polarizers based on 40 nm line/78 nm space nanowire grids", APL 90, 061104 (2007).
- [4] Yang, Z.Y. and Lu, Y.F., "Broadband nanowire-grid polarizers in ultraviolet-visible-near-infrared regions", Optics Express 15, 9510 (2007).
- [5] Berets, S., Applications Engineer, Harrick Scientific Products, personal communications, Mar. 12 - April 25, (2013).
- [6] Herzinger et al., "Ellipsometric determination of optical constants for silicon and thermally grown silicon dioxide via a multi-sample, multi-wavelength, multi-angle investigation," JAP 83, 3323-3336 (1998).